

Direct observation of a positive spin polarization at the (111) surface of magnetite

A. Pratt,^{1,2} M. Kurahashi,¹ X. Sun,^{1,3} D. Gilks,² and Y. Yamauchi¹

¹National Institute for Materials Science, 1-2-1 Sengen, Tsukuba, Ibaraki 305-0047, Japan

²York Institute for Materials Research, Department of Physics, University of York, York YO10 5DD, United Kingdom

³University of Science and Technology of China, Hefei, Anhui 230026, China

(Received 2 February 2012; revised manuscript received 8 May 2012; published 25 May 2012)

We report direct experimental evidence showing that the spin polarization P at the surface of clean $\text{Fe}_3\text{O}_4(111)$ is positive at the Fermi level E_F as measured using a spin-polarized metastable helium beam [$\text{He}(2^3S)$] and a bulk $\text{Fe}_3\text{O}_4(111)$ single crystal under high magnetic fields of up to 4 T. Density functional theory calculations confirm this surprising result, which has significant implications for the incorporation of magnetite in spintronic device applications. We also find that passivation of the surface with hydrogen does not enhance $P(E_F)$, unlike for the $\text{Fe}_3\text{O}_4(001)$ surface, where a marked increase is observed.

DOI: [10.1103/PhysRevB.85.180409](https://doi.org/10.1103/PhysRevB.85.180409)

PACS number(s): 75.70.Rf, 73.20.At, 75.47.Lx, 79.20.Rf

The spin polarization at the surface of magnetite (Fe_3O_4) is of huge technological and fundamental importance. Predictions of half-metallic ferromagnetism (HMF) and a Curie temperature which greatly exceeds that of other candidate materials have led to intensive efforts to incorporate Fe_3O_4 into spintronic devices such as magnetic tunnel junctions.^{1–3} Its use may circumvent the interfacial dipole problem encountered with, for example, manganite-based devices,⁴ and when forming an interface with Fe, Fe_3O_4 exhibits unusual antiferromagnetic exchange coupling.⁵ Additionally, at temperatures below ~ 125 K, Fe_3O_4 undergoes a unique structural transformation known as the Verwey transition.^{6,7} The (111) surface of Fe_3O_4 is in particular noted for its many technological applications⁸ and interesting polar nature,⁹ however, it is still lacking a detailed understanding. Here we report data that show the spin polarization at the surface of $\text{Fe}_3\text{O}_4(111)$ to be *positive*, as measured using a spin-polarized metastable helium beam. This result is unexpected given that the bulk spin polarization of magnetite is predicted to be -100% . However, it goes some way toward explaining the poor performance of Fe_3O_4 -based devices while also revealing significant insight into the surface electronic structure of magnetite.

The [111] crystal direction of Fe_3O_4 consists of repeating units of six atomic planes of either O^{2-} anions or Fe^{3+} and Fe^{2+} cations located at tetrahedral or octahedral sites in an inverse spinel structure. The stacking sequence of these planes has been defined in the literature as $\text{Fe}_{\text{tet}1}$, O1, $\text{Fe}_{\text{oct}1}$, O2, $\text{Fe}_{\text{tet}2}$, and $\text{Fe}_{\text{oct}2}$, as depicted in Fig. 1(b). Structural analysis using scanning tunneling microscopy^{10,11} and density functional theory (DFT) calculations¹² has shown that $\text{Fe}_{\text{tet}1}$ is the most stable surface termination with a strong relaxation in the [111] direction (the “regular” termination). Further spin-polarized photoemission spectroscopy (SPES) experiments by Dedkov *et al.* measured the spin polarization at the Fermi level $P(E_F)$ to be -80% at the surface of $\text{Fe}_3\text{O}_4(111)$ films prepared by the *in situ* oxidation of epitaxial Fe(110). This was taken as evidence for a HMF state^{13,14} with spin waves at the surface, suggested as causing a reduction in $P(E_F)$ from its intrinsic bulk value. However, the effects of surface stoichiometry and reconstruction were not discussed in detail.

In the experiments reported here, we have used a beam of electron-spin-polarized helium atoms prepared in the

metastable 2^3S state which has an energy of 19.82 eV. The deexcitation cross section for $\text{He}(2^3S)$ atoms is extremely large, preventing any penetration of the beam below the outermost surface. This is in contrast to photoemission where even low-energy UV photons ($h\nu = 21.2$ eV) generate photoelectrons that originate from below the topmost layer. When approaching to within $\sim 2\text{--}5$ Å of the surface, deexcitation of $\text{He}(2^3S)$ atoms takes place via the two-stage mechanism of resonant ionization (RI) followed by Auger neutralization (AN), resulting in the emission of a surface electron [see Fig. 1(a)]. Detecting the spin-dependent energy distribution of these ejected electrons therefore allows an extremely surface sensitive probe of the spin-split density of states (DOS) and consequently $P(E_F)$.

In determining $P(E_F)$, corrections due to the Fermi velocity and spin relaxation times may be neglected, yielding the simple definition $P(E_F) = (n_\uparrow - n_\downarrow)/(n_\uparrow + n_\downarrow)$, where $n_{\uparrow,\downarrow}$ are densities of state at E_F for majority and minority spins, respectively.¹⁵ Here, a superconducting magnet was used to apply fields of up to 4 T to the sample during measurements. Therefore, to probe $P(E_F)$, the sample current induced by electron emission $I_\uparrow(I_\downarrow)$ for $\text{He}(2^3S)$ atom spin magnetic moments aligned parallel (antiparallel) to the applied magnetic field H was measured as a function of sample bias V_S [see Fig. 1(a)].^{16,17} Then, as outlined in Ref. 18, the spin asymmetry A , defined as

$$A(V_S) = \frac{I_\uparrow(V_S) - I_\downarrow(V_S)}{I_\uparrow(V_S) + I_\downarrow(V_S)}, \quad (1)$$

gives a direct measure of the spin polarization at the Fermi level where $A(V_{S,\text{max}}) \approx -P(E_F)$. The opposite polarity of the two parameters derives from the dynamics of the AN process in which the surface electron neutralizing the $\text{He}^+(1s)$ hole must have a spin opposite to the He^+ ion. The high-energy cutoff $V_{S,\text{max}}$ occurs when the sample current due to $\text{He}(2^3S)$ deexcitation falls to zero and arises when both electrons involved in the AN process originate from the Fermi level of the substrate.

Naturally grown single crystals of $\text{Fe}_3\text{O}_4(100)$ and $\text{Fe}_3\text{O}_4(111)$ were prepared in a UHV chamber with a base pressure of $<1 \times 10^{-8}$ Pa following established procedures. After degassing the bulk crystal, a clean (100) surface was

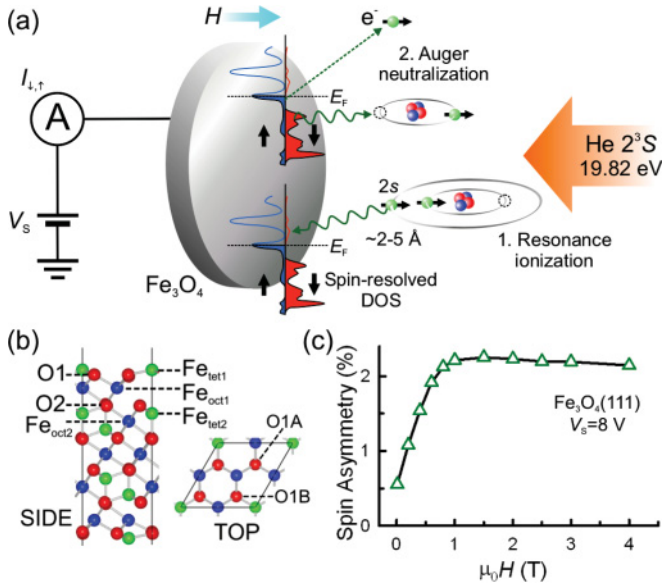


FIG. 1. (Color online) (a) Schematic of $\text{He}(2^3\text{S})$ deexcitation at the surface of Fe_3O_4 and the sample current method used to obtain the spin asymmetry, A . (b) Schematic of the surface structure of $\text{Fe}_{\text{tet}1}$ -terminated $\text{Fe}_3\text{O}_4(111)$ which corresponds to the most stable or “regular” termination. Fe_{tet} and Fe_{oct} layers represent tetrahedrally and octahedrally coordinated Fe atoms, respectively. Two O sites are present at the surface: O1A, where the O atoms bonds with three Fe_{oct} atoms, and O1B, where two Fe_{oct} bonds and one Fe_{tet} bond are formed. (c) Spin asymmetry as a function of magnetic field for a clean $\text{Fe}_3\text{O}_4(111)$ surface showing saturation at around 0.9 T ($V_s = 8$ V, $T = 83$ K).

obtained using several cycles of Ne^+ sputtering for 15 min (1 keV), followed by annealing at 300 °C for 15 min in an O_2 environment of $P_{\text{O}_2} \sim 3 \times 10^{-4}$ Pa. This produced a surface that was free from contamination within the limits of Auger electron spectroscopy, and which displayed a low-energy electron diffraction (LEED) pattern corresponding to the expected $(\sqrt{2} \times \sqrt{2})R45^\circ$ reconstruction. Following this initial cleaning procedure, the O_2 annealing step alone was sufficient to repeatedly produce the desired clean surface. The preparation of the (111) surface followed the same procedure except that an annealing temperature of 550 °C was used and that, prior to each experiment, several sputter and anneal cycles were necessary to obtain a sharp hexagonal LEED pattern, which in this case indicated a (2×2) reconstruction. Hydrogen-terminated surfaces were prepared using a homemade atomic hydrogen source to achieve saturation.¹⁸

Figure 1(c) shows the dependence of the spin asymmetry on the applied magnetic field for an $\text{Fe}_3\text{O}_4(111)$ surface at 83 K. A saturates just before 1 T and then plateaus, consistent with the Fe_3O_4 saturation magnetization of ~ 0.9 T. A similar trend was also observed at temperatures up to 298 K, although the magnitude of the asymmetry monotonically decreased slightly with increasing temperature. Previous measurements for $\text{Fe}_3\text{O}_4(001)$ thin films showed a gradual increase in A at fields greater than 1 T due to the presence of antiphase boundaries¹⁹ which prevent true saturation¹⁸ and are absent for the single crystals used here. The dependence of the measured sample current on V_s for clean $\text{Fe}_3\text{O}_4(111)$ is shown

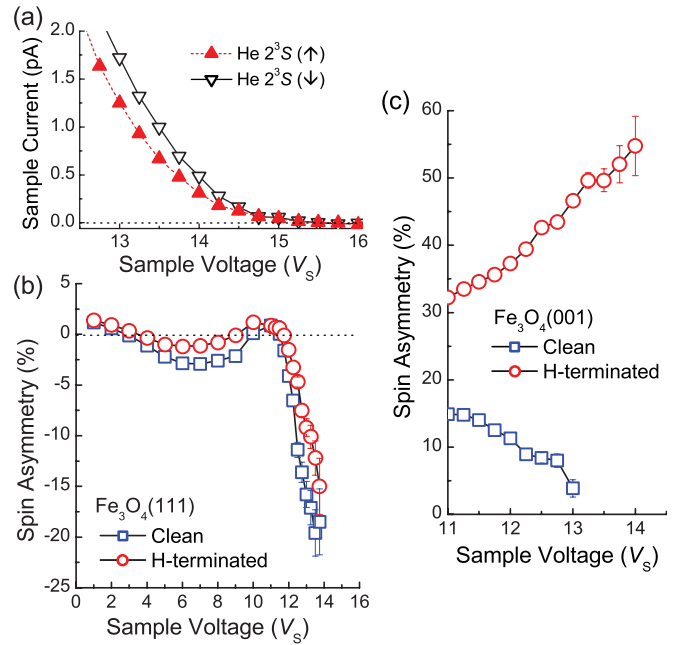


FIG. 2. (Color online) (a) The dependence of the sample current, induced by $\text{He}(2^3\text{S})$ deexcitation, on applied sample voltage for clean $\text{Fe}_3\text{O}_4(111)$ ($\mu_0 H = 4$ T, $T = 298$ K). A clear difference in signal is observed for $\text{He}(2^3\text{S})$ spins aligned parallel (\uparrow) and antiparallel (\downarrow) to the applied field direction. $V_{s,\text{max}}$ occurs when the measured sample current due to $\text{He}(2^3\text{S})$ deexcitation falls to zero. The corresponding spin asymmetry is shown in (b), along with that for the hydrogen-terminated surface. Hydrogen adsorption has little effect on the spin asymmetry unlike for the (001) surface, (c), where a drastic enhancement is observed.

in Fig. 2(a). In these spectra, corrections due to a small photon contribution¹⁷ and $\text{He}(2^3\text{S})$ -induced desorption of positive ions²⁰ have been made. The corresponding spin asymmetry is shown in Fig. 2(b), where it is clear that on approaching $V_{s,\text{max}}$, A rapidly decreases to $< -20\%$. This directly indicates that the spin polarization for the $\text{Fe}_{\text{tet}1}$ termination of $\text{Fe}_3\text{O}_4(111)$ is *positive* at the Fermi level. Hydrogen termination has little effect on the asymmetry, resulting in a small shift toward a more positive value. For comparison, Fig. 2(c) shows the spin asymmetry for a clean and hydrogen-terminated $\text{Fe}_3\text{O}_4(001)$ surface. Here, the spin asymmetry of the clean surface is very slightly positive and is greatly enhanced after the adsorption of hydrogen to $> 50\%$. This pronounced effect, obtained using a single crystal $\text{Fe}_3\text{O}_4(001)$ sample, confirms our previous measurements of A for $\text{Fe}_3\text{O}_4(001)$ thin films^{18,21} and is well understood based on knowledge of the modified $\text{Fe}(B)$ -terminated (001) surface.^{22–24}

The result of a positive spin polarization for the (111) surface is altogether more surprising and for further understanding we have conducted DFT calculations using the Vienna *ab initio* simulation package.²⁵ A fully relaxed 17-layer slab consisting of six Fe_{tet} , five Fe_{oct} , and six O layers was used to represent the surface with a vacuum region of 16.4 Å. Tests showed that increasing the vacuum gap and/or number of atomic layers in the slab produced consistent results to those presented. Both sides of the slab were terminated with $\text{Fe}_{\text{tet}1}$ atoms to represent the experimentally prepared surface.

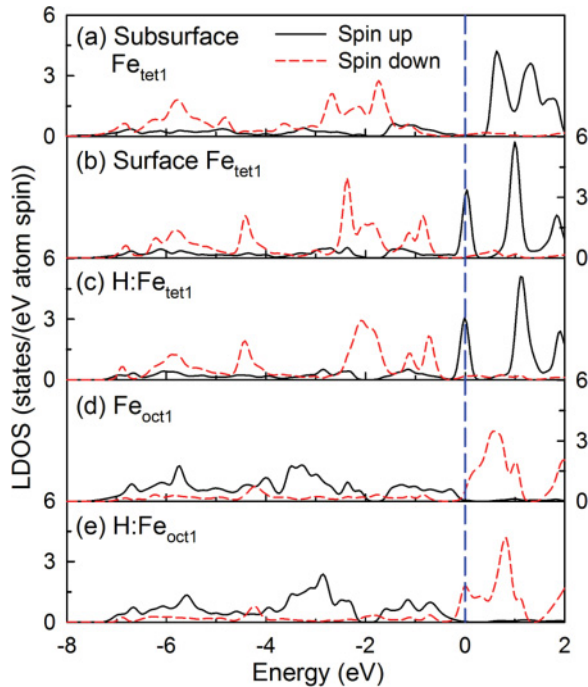


FIG. 3. (Color online) LDOS of $\text{Fe}_{\text{tet}1}$ atoms located (a) subsurface and (b) at the surface of the most stable structure, as depicted in Fig. 1(b). Majority spin-up states that are empty in the bulk are partially filled at the surface leading to a positive spin polarization at the Fermi level, E_F . Hydrogen adsorption has little effect on surface $\text{Fe}_{\text{tet}1}$ atoms as shown in (c). (d) and (e) show equivalent LDOS for $\text{Fe}_{\text{oct}1}$ atoms at clean and hydrogen-terminated $\text{Fe}_3\text{O}_4(111)$ surfaces, respectively.

Figures 3(a) and 3(b) show spin-resolved local DOS (LDOS) calculations for $\text{Fe}_{\text{tet}1}$ atoms located below the surface and in the terminating layer, respectively. It is clear that majority spin-up states that are empty in the bulk become partially occupied at the surface, leading to a sharp peak and positive spin polarization at E_F . Empty $3d_{z^2}$ states overwhelmingly contribute to this modification.²⁶ Qualitatively, these changes originate from the reduced valency of $\text{Fe}_{\text{tet}1}$ atoms which are only bonded to three O ions at the surface as opposed to four in the bulk. The extra charge associated with this reduced coordination partially occupies the $\text{Fe}_{\text{tet}1}$ majority band as the minority band is already filled, leading to a positive spin polarization at E_F as we observe experimentally. It should be noted that the LDOS results presented in Fig. 3 do not change significantly when the on-site Coulomb interaction term $+U$ is considered.²⁶

For hydrogen termination, DFT calculations show that adsorption is energetically favored at O atoms in the outermost O1 layer that are otherwise only bonded to $\text{Fe}_{\text{oct}1}$ atoms [identified in Fig. 1(b) as O1A]. Atoms at the alternative O1B site have two bonds to bulklike $\text{Fe}_{\text{oct}1}$ atoms in the layer below and one bond to a surface $\text{Fe}_{\text{tet}1}$ atom which, as discussed above, is itself uncompensated. The partial charge saturation arising from this O1B- $\text{Fe}_{\text{tet}1}$ bond yields a positive spin polarization and results in a lack of surface states. In contrast, surface states are present at the O1A site, meaning that hydrogen preferentially adsorbs to these atoms and consequently has little effect on the terminating $\text{Fe}_{\text{tet}1}$

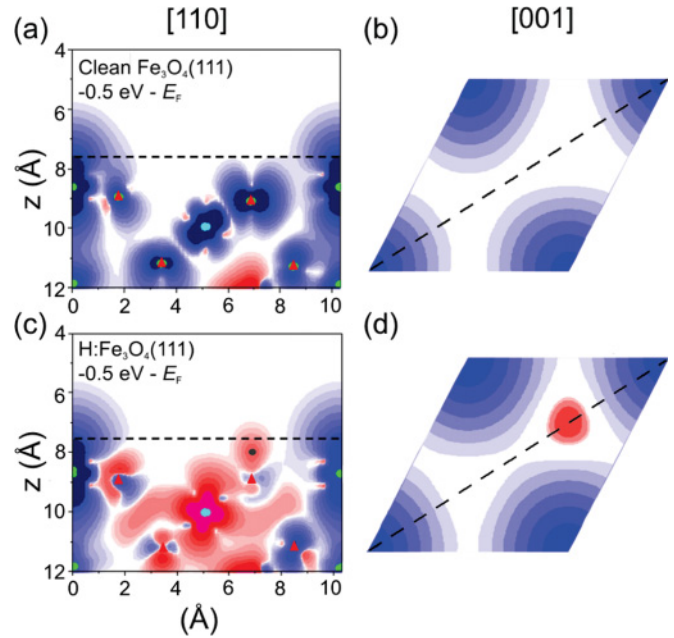


FIG. 4. (Color online) Maps of spin density in planes representing side ([110]) and top ([001]) views of clean and hydrogen-terminated $\text{Fe}_3\text{O}_4(111)$ surfaces [see Fig. 1(b)]. The [001] planes are located 1 Å above the outermost $\text{Fe}_{\text{tet}1}$ layer, as indicated by horizontal dashed lines in (a) and (c). The diagonal lines in (b) and (d) correspond to the [110] planes shown in (a) and (c). $\text{Fe}_{\text{tet}1}$ and $\text{Fe}_{\text{oct}1}$ atoms are represented by green and blue circles, respectively, O atoms by red triangles, and H atoms by gray circles. A darker blue (red) color indicates more dominant majority (minority) spin states.

layer, as shown in the LDOS of Fig. 3(c). The slight reduction in the magnitude of the spin asymmetry that is observed in Fig. 2(b) is due to the modification of the DOS of the outermost $\text{Fe}_{\text{oct}1}$ atoms as seen in Figs. 3(d) and 3(e), which show that hydrogen termination increases the minority states at E_F . It is also clear from the LDOS results of Fig. 3 that coupling between atomic magnetic moments in the tetrahedral and octahedral sublattices is antiparallel. This results in a change in the polarity of the spin polarization at the surface depending on the terminating sublattice and gives rise to the ferrimagnetism of Fe_3O_4 .

To visually summarize the above deductions, spin density maps along the [110] and [001] directions of $\text{Fe}_{\text{tet}1}$ -terminated $\text{Fe}_3\text{O}_4(111)$ are shown in Fig. 4 for clean and hydrogen-adsorbed surfaces. Calculations incorporating DOS from -0.5 eV to E_F are displayed with the (001) planes in Figs. 3(b) and 3(d) located at 1 Å above the outermost $\text{Fe}_{\text{tet}1}$ layer. It is clear from these plots that in the region around E_F , the spin polarization at the vacuum side is positive supporting our experimental observation. Hydrogen termination leads to a small reduction in the magnitude of the positive spin polarization, effectively “opening up” the outermost $\text{Fe}_{\text{oct}1}$ layer so that incoming $\text{He}(2^3S)$ atoms are able to access these electronic states. This in turn leads to the observed reduction in the magnitude of the spin asymmetry.

Our results indicate that the spin polarization at the most stable termination of $\text{Fe}_3\text{O}_4(111)$ is positive and $>20\%$ at E_F . This is opposite in polarity to the values measured by

previous photoemission experiments, which yielded -80% for $P(E_F)$.^{13,14} Yet the two results are not contradictory, arising instead from the different penetration depths of the probe beams used in each study. The surface sensitivity of He(2^3S) atoms ensures that only electronic states of the outermost Fe_{tetl} layer contribute to the measured signal. In contrast, UV photoemission will yield a signal that is averaged over the DOS of several atomic layers including octahedrally coordinated Fe layers below the surface which have a spin polarization much closer to the bulk value that is predicted to be -100% . Hence, taking a value for $P(E_F)$ as measured by photoemission to be an “intrinsic” parameter is flawed and more consideration of the drastic changes in electronic structure that can occur at a surface is needed. In contrast, our results suggest that the stable (001) and (111) surfaces of Fe₃O₄ do have an intrinsic spin polarity which differs greatly from the bulk. This has significant consequences in terms of device applications as one of the motivating factors for the use of Fe₃O₄ is its high spin polarization. We note here that our experiments were performed with naturally grown single crystals so that there

is no question as to the quality of the prepared surface which may not be the case for thin film samples.

In summary, we have measured a strong *positive* spin polarization at the stable Fe_{tetl}-terminated surface of Fe₃O₄(111). This unexpected finding could explain the reduced magnetoresistance and lack of reproducibility observed with spintronic devices based on this crystallographic orientation. A more promising route to taking advantage of the natural properties of Fe₃O₄ may be to use the (001) orientation as at this surface $P(E_F)$ may be greatly enhanced through, for example, passivation with hydrogen. Revealing such drastic changes in the surface electronic structure of Fe₃O₄ also suggests that other ferrimagnetic compound crystal surfaces require further investigation.

This research was supported by a Ministry of Education, Science, Sports and Culture Grant-in-Aid for challenging Exploratory Research (Grant No. 23656034). A.P. acknowledges financial support from the Japan Society for the Promotion of Science.

-
- ¹P. Seneor, A. Fert, J.-L. Maurice, F. Montaigne, F. Petroff, and A. Vaurès, *Appl. Phys. Lett.* **74**, 4017 (1999).
²G. Hu and Y. Suzuki, *Phys. Rev. Lett.* **89**, 276601 (2002).
³T. Kado, *Appl. Phys. Lett.* **92**, 092502 (2008).
⁴M. Minohara, R. Yasuhara, H. Kumigashira, and M. Oshima, *Phys. Rev. B* **81**, 235322 (2010).
⁵T. Kida, S. Honda, H. Itoh, J. Inoue, H. Yanagihara, E. Kita, and K. Mibu, *Phys. Rev. B* **84**, 104407 (2011).
⁶E. J. W. Verwey, *Nature (London)* **144**, 327 (1939).
⁷M. S. Senn, J. P. Wright, and J. P. Attfield, *Nature (London)* **481**, 173 (2012).
⁸W. Weiss and W. Ranke, *Prog. Surf. Sci.* **70**, 1 (2002).
⁹V. K. Lazarov, S. A. Chambers, and M. Gajdardziska-Josifovska, *Phys. Rev. Lett.* **90**, 216108 (2003).
¹⁰T. K. Shimizu, J. Jung, H. S. Kato, Y. Kim, and M. Kawai, *Phys. Rev. B* **81**, 235429 (2010).
¹¹M. Paul, M. Sing, R. Claessen, D. Schrupp, and V. A. M. Brabers, *Phys. Rev. B* **76**, 075412 (2007).
¹²M. E. Grillo, M. W. Finnis, and W. Ranke, *Phys. Rev. B* **77**, 075407 (2008).
¹³Y. S. Dedkov, U. Rüdiger, and G. Güntherodt, *Phys. Rev. B* **65**, 064417 (2002).
¹⁴M. Fonin, Y. S. Dedkov, R. Pentcheva, U. Rüdiger, and G. Güntherodt, *J. Phys.: Condens. Matter* **20**, 142201 (2008).
¹⁵P. A. Dowben, N. Wu, and C. Binek, *J. Phys.: Condens. Matter* **23**, 171001 (2011).
¹⁶M. Kurahashi, T. Suzuki, and Y. Yamauchi, *Appl. Phys. Lett.* **85**, 2869 (2004).
¹⁷M. Kurahashi and Y. Yamauchi, *Rev. Sci. Instrum.* **79**, 073902 (2008).
¹⁸M. Kurahashi, X. Sun, and Y. Yamauchi, *Phys. Rev. B* **81**, 193402 (2010).
¹⁹D. T. Margulies, F. T. Parker, M. L. Rudee, F. E. Spada, J. N. Chapman, P. R. Aitchison, and A. E. Berkowitz, *Phys. Rev. Lett.* **79**, 5162 (1997).
²⁰M. Kurahashi and Y. Yamauchi, *Phys. Rev. Lett.* **84**, 4725 (2000).
²¹A. Pratt, M. Kurahashi, X. Sun, and Y. Yamauchi, *J. Phys. D: Appl. Phys.* **44**, 064010 (2011).
²²M. Fonin, R. Pentcheva, Y. S. Dedkov, M. Sperlich, D. V. Vyalikh, M. Scheffler, U. Rüdiger, and G. Güntherodt, *Phys. Rev. B* **72**, 104436 (2005).
²³R. Pentcheva, F. Wendler, H. L. Meyerheim, W. Moritz, N. Jedrecy, and M. Scheffler, *Phys. Rev. Lett.* **94**, 126101 (2005).
²⁴G. S. Parkinson, N. Mulakaluri, Y. Losovyj, P. Jacobson, R. Pentcheva, and U. Diebold, *Phys. Rev. B* **82**, 125413 (2010).
²⁵G. Kresse and J. Furthmüller, *Phys. Rev. B* **54**, 11169 (1996).
²⁶See Supplemental Material at <http://link.aps.org/supplemental/10.1103/PhysRevB.85.180409> for Fe *d* orbital contributions to the calculated LDOS shown in Fig. 3(a) and for data showing the effect of the on-site Coulomb interaction term *U*.